Investigation of Cyclic Loading of Aged Piles in Sand

David Igoe[1] and Kenneth Gavin[2]

Abstract: In recent years, there has been a significant push to develop optimized pile designs in the offshore industry, driven by the growth of offshore wind. One of the largest remaining uncertainties governing axial pile design in sands is the influence of ageing effects and how an aged pile responds under axial cyclic loading. This paper presents results from a long-term campaign of field tests on pile ageing and axial cyclic loading in sands, undertaken at the Blessington geotechnical test site in Ireland. Five open-ended driven steel piles were subjected to a total of 33 static and cyclic tension pile load tests undertaken over a 3-year period. The tests were planned and coordinated in order to accurately quantify the effects of ageing and cyclic loading on the pile shaft capacity over time. The tests showed that significant gains in pile shaft capacity occurred over time as a result of pile ageing, in line with results presented by other researchers. Piles subjected to cyclic tension loading remained stable under cyclic loading at load levels much larger than their 1-day capacity. The 1-day capacity appears to offer a lower bound for the degraded pile capacity following tension cyclic loading to failure. The reduction in capacity caused by cyclic loading to failure was related to the pretest increase in capacity caused by ageing. The findings from these field tests in addition to reinterpretation of previous testing indicated that previously published cyclic interaction boundaries may be overly conservative. **DOI: 10.1061/(ASCE)GT.1943-5606.0002451.**

Author keywords: Offshore piles; Axial pile capacity; Pile ageing; Cyclic loading; Sand.

Introduction

As the offshore wind industry expands and moves into less favorable sites with deeper waters, there is a need to continuously improve engineering design approaches to ensure costs remain viable. In water depths greater than 40 m, piled jacket structures are the most common substructure used to support offshore wind turbines (OWTs). These structures primarily rely on axial pile capacity to resist the applied loading, and therefore axial tension and compression capacity will govern the pile length. The shaft capacity of piles in sand has been described as a moving target (Jardine and Chow 2007), where significant capacity increases, known as pile ageing, have been observed within the first few months following installation (York et al. 1994; Axelsson 2000; Bullock et al. 2005; Jardine et al. 2006; and others). The majority of piled foundations experience both ageing and cyclic loading in some form, particularly for offshore wind structures where environmental loading from wind and wave forces are substantial, but the potential effects of these are often ignored in design (Jardine and Standing 2012). Adopting pile ageing factors in design could lead to shorter piles with the associated cost savings as well as reduced installation risk (Manceau et al. 2019). For a typical offshore wind farm, there will be several months' delay between the installation of the jacket piles and the installation and commissioning of the turbine. Despite the widely accepted evidence of the beneficial effects of pile ageing from numerous sources, there has been a reluctance in the industry to include pile ageing in design or to incorporate pile ageing factors in design standards. This is partly due to conservatism within the industry and the slow adoption of new design approaches but mainly due to a lack of full-scale data to verify these aged capacities and a poor understanding of the mechanisms controlling the ageing process. In addition, there is very little test data available on the effects of cyclic loading of aged piles in sands and significant uncertainty with regard to the axial capacity degradation caused by cyclic loading on aged piles. Accurately predicting the axial cyclic loading response of driven piles is particularly challenging due to the complex soil stress history at the pile–soil interface. Manceau et al. (2019) described the design of jacket piles for the Beatrice offshore wind farm in the UK where ageing capacity gains were not considered as part of the baseline pile length calculations because of the assertion that ageing effects can be brittle and prevented by high-amplitude cycling. However, some limited allowances for pile ageing effects were used as part of a mitigation strategy in case of pile driving refusal to offset some of the shaft capacity degradation if drilling was required. This was justified by an assessment of the cyclic loading that would be experienced by a pile over a 200-day period prior to installation of the wind turbine, which was deemed not to have a detrimental effect on pile capacity or prevent pile ageing. It is clear that a greater understanding of cyclic loading effects on aged piles in sand is required if pile ageing factors are to be widely adopted for jacket pile design.

Pile Installation and Ageing

Over the last 20 years, numerous research studies have been undertaken to better understand the mechanisms controlling driven pile behavior in sand. Lehane et al. (1993) proposed that the pile shaft resistance can be characterized by a Coulomb failure criteria, where the local shear stress at failure τ_f is dependent on the radial effective stress at the pile–soil interface at failure σ'_{rf} and the interface friction angle between the pile material and soil δ_f [Eq. (1)]. The radial stress at failure σ'_{rf} can be further separated into equalized

[1]Assistant Professor, Dept. of Civil, Structural and Environmental Engineering, Univ. of Dublin, Trinity College D02PN40, Dublin 2, Ireland (corresponding author). ORCID: https://orcid.org/0000-0003-3283-2947. Email: igoed@tcd.ie

[2]Professor of Subsurface Engineering, Geo-Engineering Section, Faculty of Civil Engineering and Geosciences, Delft Univ. of Technology, Bldg. 23, Stevinweg 1, P.O. Box 5048, 2628 CN Delft, Netherlands.

Note. This manuscript was submitted on June 19, 2019; approved on September 15, 2020; published online on February 15, 2021. Discussion period open until July 15, 2021; separate discussions must be submitted for individual papers. This paper is part of the ***Journal of Geotechnical and Geoenvironmental Engineering***, © ASCE, ISSN 1090-0241.

radial stress values σ'_{rc} and the change in radial stress due to dilation and principal stress rotation during shearing $\Delta\sigma'_r$

$$\tau_f = \sigma'_{rf} \cdot \tan\delta_f = (\sigma'_{rc} + \Delta\sigma'_r) \cdot \tan\delta_f \quad (1)$$

As a displacement pile is installed in sand, the stresses beneath the pile tip can increase by several orders of magnitude relative to the in-situ conditions (White 2005), resulting in considerable crushing of the underlying sand particles as the pile tip approaches (White and Bolton 2001). As the pile tip advances, the sand is displaced laterally and passes around the pile tip, undergoing large reductions in the radial stresses in the process. Yang et al. (2010), using laboratory model pile testing, identified different zones of material around the shear band, characterized by different levels of particle crushing. The sand along the pile shaft is subjected to repeated cyclic shearing as the pile advances, resulting in a shear zone of varying thickness and a shear band in which the particles are aligned along the pile soil interface.

Following installation, before the main structure is assembled, there will be an ageing period where the applied loading will be small relative to the extreme design loads. The phenomenon of soil ageing in clean sands is well established, whereby an increase in strength and stiffness occurs after deposition or densification (e.g. Mitchell and Solymar 1984; Dumas and Beaton 1988; Jefferies et al. 1988; Schmertmann 1992; and others). This is thought to be due to two main mechanisms:

1. Increased friction due to secondary compression, increased interlocking of particles, and internal stress arching (Mesri et al. 1990; Schmertmann 1992); and
2. Increased cementation and cohesion as a result of chemical processes such as the dissolution and precipitation of silica or calcium carbonate at particle contacts (Mitchell and Solymar 1984; Baxter and Mitchell 2004).

The mechanisms of pile ageing are less well known, although notable developments have been made in recent years (Jardine et al. 2006; Rimoy et al. 2015; Lim and Lehane 2015; Gavin et al. 2013, 2015; Gavin and Igoe 2019; and others). Chow et al. (1998) considered three possible mechanisms for pile ageing:

1. Changes in the stress regime leading to increase in equalized radial stress σ'_{rc}.
2. Ageing of the disturbed soil leading to increased constrained dilation $\Delta\sigma'_r$.
3. Chemical corrosion resulting in an increased pile surface roughness and interface friction angle δ_f.

As part of a long-term field investigation into pile ageing, Gavin et al. (2013) and Gavin and Igoe (2019) presented results from the installation, ageing, load-testing, and extraction of field-scale driven piles in Blessington, which are directly related to the field tests discussed in this paper. Based on these findings and previous work by other researchers, the authors suggest the primary mechanisms for pile ageing are increased constrained dilation (Mechanism B) and physiochemical processes (Mechanism C), resulting in cementation of the shear zone formed during pile driving. A "fresh" (un-aged) pile will experience shear failure at the pile–soil interface. The sand contained within the shear zone will have experienced extreme cyclic shearing, particle realignment, and grain crushing during driving (due to repeated hammer blows). The sand in this zone will likely contract during tension loading (i.e., negative $\Delta\sigma'_r$), where stress reversals cause a rotation of principal stresses, resulting in low end-of-driving shear stresses and shaft capacity. Over time, physiochemical processes, accelerated by particle breakage, such as the dissolution and precipitation of silica (Mitchell and Solymar 1984; Baxter and Mitchell 2004), can cause cementation of the sand in the shear zone. When axially loaded to failure, the shear failure zone moves into the sand mass, increasing the friction angle of the shear zone from the soil–steel interface value to a soil–soil value. In addition, creep-induced stress redistribution can lead to increased particle interlocking, resulting in increased dilation and large increases in radial stress during shearing (i.e., large positive $\Delta\sigma'_r$). The combination of processes can ultimately result in an up to threefold increase in shaft resistance.

Cyclic Loading

There have been ongoing efforts to improve cyclic axial pile design in sands, with the most notable contributions from Imperial College London (ICL), Institut National Polytechnique de Grenoble (INPG), and others on the grouted offshore piles alternating loading (GOPAL) and piles under cyclic solicitations (SOLCYP) research projects (Jardine and Standing 2012; Tsuha et al. 2012; Rimoy et al. 2013; Puech et al. 2013). The cyclic response of piles in sand has been shown by Tsuha et al. (2012) to be primarily affected by the number (N) of load cycles, the mean cyclic load Q_{mean}, and cyclic amplitude Q_{cyc} (Fig. 1) relative to the static capacity immediately preceding the test $Q_{s(t)}$, among other factors. The dearth of field cyclic tests on driven piles in sand was highlighted by Jardine et al. (2012), who noted that there were 14 case histories for axial cyclic loading of driven piles in clay but only a single field-scale case history in silica sand. Field scale tests are essential to develop our understanding of pile behavior because numerous lab studies have failed to capture the ageing trends noted in the field (Carroll et al. 2019; Rimoy et al. 2015). To date, our main understanding of the combined effects of ageing and cyclic loading on the capacity of driven piles in sands stems from the GOPAL pile test campaign in Dunkirk that investigated the combined effects of ageing and cyclic loading on the capacity of driven piles in sands (Jardine et al. 2006; Jardine and Standing 2012, 2000). The tests involved numerous static and cyclic tests on seven 457-mm-diameter steel piles driven into the dense marine sand deposit at Dunkirk. The piles were tested sequentially over time to investigate both the intact ageing characteristics of the pile and the effects of cyclic loading on the pile capacity. The field tests confirmed the laboratory finding of Tsuha et al. (2012) showing that low-level "stable" cycling, where the pile head displacements accumulate slowly or plateau over hundreds of cycles, could increase the shaft capacity. High-level "unstable" cycling, where head displacements develop rapidly, leading to failure within 100 cycles, could markedly degrade the shaft capacity. Intermediate "metastable" behavior describes where pile

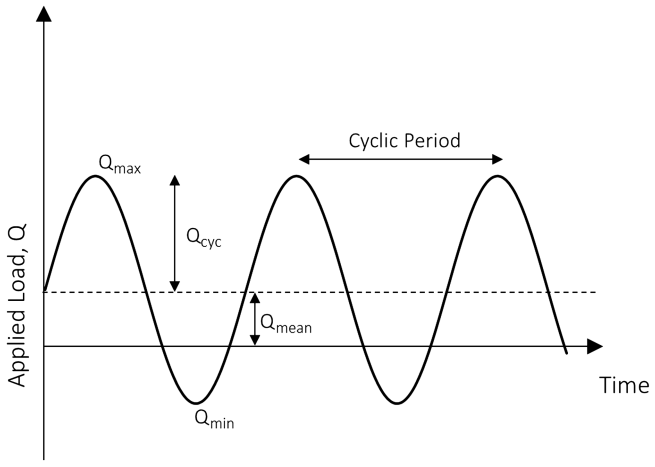

Fig. 1. Definition of cyclic loading parameters.

head displacements accumulate at moderate rates over tens to hundreds of cycles without stabilizing and cyclic failure develops within $100 < N < 1{,}000$. The limited number of piles and wide range of cyclic loading combinations led to multiple tests being performed on the same piles. The influence of prior testing history was accounted for by tracking changes in the tension capacity; however, unavoidable ambiguities were acknowledged by the authors (Jardine and Standing 2012). The analysis of the Dunkirk tests led to the development of cyclic interaction diagrams (discussed later) and a widely used global pile approach for estimating the average degradation of shaft capacity due to cyclic loading. The Jardine and Standing (2012) approach for estimating cyclic degradation stems from the Imperial College pile (ICP) design guidelines (Jardine et al. 2005), which expresses the change in local radial stress acting on the pile shaft due to cyclic loading $\Delta\sigma'_{r,\mathrm{cyc}}$ as

$$\frac{\Delta\sigma'_{r,\mathrm{cyc}}}{\sigma'_{rc}} = A\left(B + \frac{\tau_{\mathrm{cyc}}}{\tau_f}\right)N^C \tag{2}$$

where τ_{cyc} = locally applied cyclic shear stress; N = number of cycles for a given load level; and A, B, and C = calibration coefficients. By conservatively ignoring the base resistance, neglecting the effect of constrained interface dilation ($\Delta\sigma'_r$) on the pile shaft, and assuming that the local reduction in shaft resistance can be applied globally to cover the average degradation of shaft resistance (ΔQ_s), Jardine and Standing (2012) proposed the following equation:

$$\frac{\Delta Q_s}{Q_{s(t)}} = A\left(B + \frac{Q_{\mathrm{cyc}}}{Q_{s(t)}}\right)N^C \tag{3}$$

Direct calibration from the Dunkirk results gives the following: $A = -0.126$, $B = -0.10$, and $C = 0.45$. A lower limit was applied for one-way cycling when $Q_{\mathrm{cyc}}/Q_{s,t} = Q_{\mathrm{mean}}/Q_{s,t} = 0.25$, below which cycling improves rather than degrades capacity. The previous approach is widely used in design practice for estimating the degradation of offshore piles, despite being based on a limited number of tests from a single site. Neglecting the effect of constrained interface dilation ($\Delta\sigma'_r$) may be a valid assumption for recently driven piles (due to its small contribution to capacity), but this assumption may no longer be valid for aged piles, where $\Delta\sigma'_r$ may have a large contribution to the shaft capacity. This paper aims to provide much-needed field test data to inform the axial design of aged piles in sand under cyclic loading. The axial capacity of five steel piles was accurately tracked using a carefully planned load testing regime that considered both ageing and cyclic effects and also the influence of testing on the capacity itself. This paper aims to fill in the gaps in the literature, namely:

- Investigate the link between ageing and the effects of cyclic loading on the pile capacity.
- Investigate the effects of testing to failure and retesting on pile capacity.
- Propose new cyclic interaction diagrams and an updated cyclic degradation approach based on the findings in this paper.

Experimental Testing at Blessington

In this paper, axial load testing on open-ended steel piles driven into a dense sand deposit near Blessington, Ireland, is described. Multiple static and cyclic loading tests performed on four steel piles, designated S2, S3, S4, and S6, are discussed in this paper. First-time "fresh" tension tests from each of these piles have been previously reported in Gavin and Igoe (2019) and Igoe et al. (2013). Tension testing was preferred over compression testing to reduce the uncertainty related to separating the shaft and base resistance components for open-ended piles. All piles had identical geometries with an outer diameter D of 340 mm, wall thickness of 14 mm, and embedded length of 7 m. Pile S6 had two diametrically opposite steel channels welded onto the outer shaft to house strain gauges, and radial stress sensors were embedded in the pile wall at locations offset circumferentially at 90° to these channels, as described in Gavin and Igoe (2019).

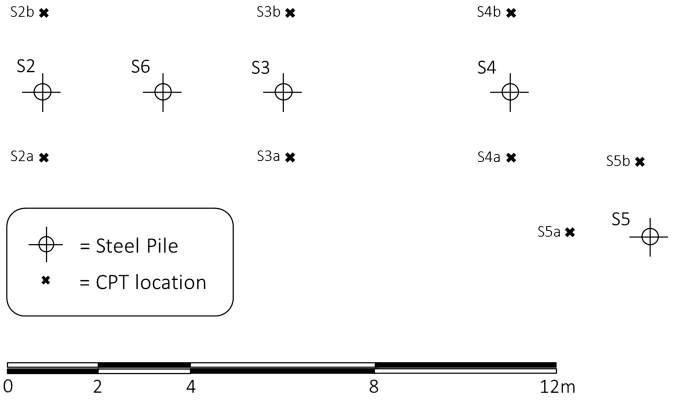

Fig. 2. Layout of test Piles S2–S6 with adjacent CPT locations.

Site Description

The pile tests were performed at the upper geotechnical test site located in the Redbog quarry in Blessington, 25 km southwest of Dublin, Ireland. The ground conditions at the site and the sand properties have been reported in Doherty et al. (2012), Igoe et al. (2011), and Igoe and Gavin (2019). Details of the site layout are shown in Fig. 2. The ground conditions were dense to very dense glacially deposited overconsolidated fine sand. Eight cone penetration tests (CPTs) were performed in the area of the pile tests (Fig. 3), and the cone resistance q_c values increased from ~10 MPa close to ground level to ~20 MPa at the pile toe 7 m below ground level (bgl). The sand had a mean particle size D_{50} between 0.1 and 0.15 mm and a fines content (percentage of clay and silt particles) of between 4% and 13%. The water table was well below the base of the piles discussed in this paper, at approximately 13 m bgl.

Pile Installation

Piles S2–S4 were driven using a Junttan PM16 pile-driving rig that had a 4-t hammer and a 0.3-m stroke. Driving was paused every 1 m in order to allow measurements of the stationary radial stress and soil plug length until the target penetration depth of 7 m bgl had been achieved. Pile S6 was driven using a Junttan PM20 piling rig with a 5-t HHK-5A hammer (Junttan Oy, Kuopio, Finland). A stroke length of 0.2 m was used for the first 4 m of installation; this was then increased to 0.35 m for the remainder of the driving process. The installation of Pile S6 was paused every 0.25 m during driving to measure the soil plug length and stationary radial stress.

The driving records for each pile are shown in Fig. 4. The total blow counts required to reach the final penetration of 7 m varied between 529 and 739 blows for Piles S2–S4 using the 4-t hammer and ~1,500 blows for Pile S6 with the 5-t hammer, albeit at a lower hammer drop height for most of the installation. The maximum energy transferred into the piles (EMX) was estimated

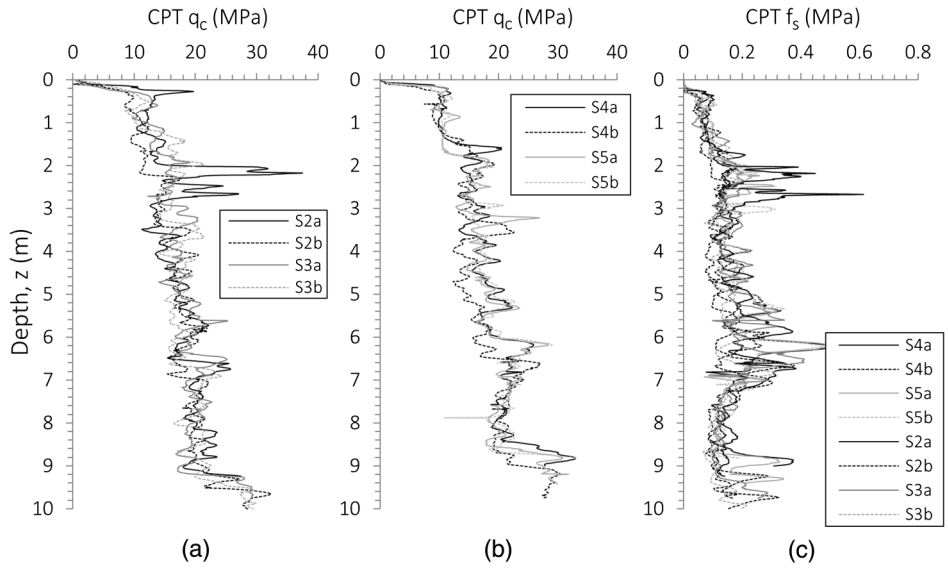

Fig. 3. Cone resistance for CPTs: (a) S2–S3; (b) S4–S5; and (c) CPT sleeve friction for all.

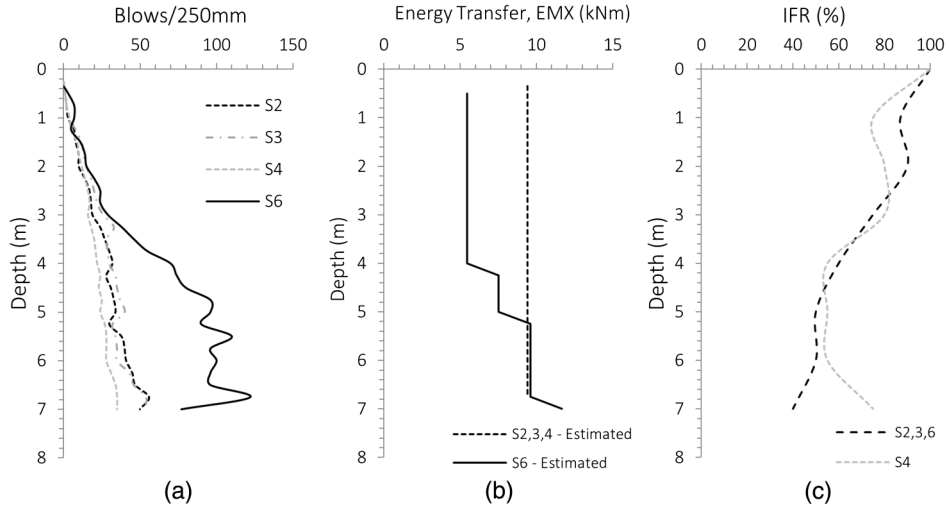

Fig. 4. Installation: (a) total cumulative blow count; (b) blows/250 mm penetration; and (c) incremental filling ratio (IFR).

using the approach adopted in Gavin and Igoe (2019), which was based on linear fit to measured EMX data for the same piling hammers from Flynn and Mccabe (2016). A comparison of the estimated EMX is provided in Fig. 4(b), and it is clear that Pile S6 has significantly lower average EMX for most of installation, which explains the significantly higher number of blows required for installation of Pile S6.

The degree of pile plugging during installation was measured for Piles S3 and S4 using the incremental filling ratio (IFR, incremental change in plug length with respect to penetration), as shown in Fig. 4(c). Due to the difficulty in measuring IFR, the plug length ratio (PLR, ratio of total plug length to pile embedded length) is often used because it can be measured at the end of installation. Piles S2, S3, and S6 developed similar PLRs with a final plug length of 4.48 + –0.02 m (PLR = 64% + –0.5%). Pile S4 had a final plug length of 4.75 m (PLR = 68%). A comparison of the IFR profiles from Piles S3 and S4 indicated that all the piles had a similar IFR profiles to 6 m bgl, below which the IFR of Pile S4 deviated and increased over the final 1 m of penetration, resulting in a final IFR ≈ 75%. The ultimate tension capacity of Pile S4 measured from static load tests (discussed later) was also significantly lower. Although the exact reason for the low capacity of Pile S4 compared with the other piles is unclear, it is postulated here that Pile S4 may have been affected by a local silt pocket at the base of the pile, which could have significantly reduced both the internal and external skin friction over the bottom few meters of the pile. This could explain the change in plugging behavior and also the much-reduced tension capacity, where the bottom 3 m of the pile provides the majority of the shaft resistance.

Load Testing Procedure

After installation, the piles were load tested in tension at various time intervals after driving. The tests were scheduled to (1) capture the ageing effects on previously untested fresh piles following driving, (2) to capture the effects of static loading retesting, and (3) to quantify the impact of cyclic loading on aged piles. Full details of the experimental testing program are provided in Table 1.

Table 1. Details of pile tests

Pile (test)	Date	Age (days)	Test type	Load (and permanent displacement)
S2	April 28, 2011	0	Driving (Junttan PM16)	695 blows (400-mm drop height)
(S2.Stat1)	April 29, 2011	1	Maintained load	Capacity = 344 kN (34 mm)
(S2.Stat2)	April 29, 2011	1	Quick load	Capacity = 332 kN (18 mm)
(S2.Cyc1)	April 29, 2011	1	Cyclic load test (20 cycles)	Load = 0–220 kN (0 mm)
(S2.Stat3)	April 29, 2011	1	Quick load	Capacity = 351 kN (16 mm)
(S2.Stat4)	May 9, 2011	11	Maintained load	Capacity = 430 kN (36 mm)
(S2.Stat5)	August 31, 2011	125	Maintained load	Capacity = 752 kN (31 mm)
(S2.Stat6)	August 31, 2011	125	Maintained load	Capacity = 600 kN (23 mm)
(S2.Cyc2)	August 31, 2011	125	Cyclic load test (170 cycles)	Load = 0–380 kN (0 mm) (stable)
(S2.Cyc3)	August 31, 2011	125	Cyclic load test (170 cycles)	Load = 0–520 kN (4.7 mm) (metastable)
(S2.Stat7)	August 31, 2011	125	Maintained load	Capacity = 600 kN, drops to 440 kN (23 mm)
S3	April 28, 2011	0	Driving (Junttan PM16)	739 blows (400 mm drop height)
(S3.Stat1)	May 09, 2011	11	Maintained load	Weld failed at 525 kN (4.1 mm)
(S3.Stat2)	May 11, 2011	13	Maintained load	Capacity = 665 kN (59 mm)
(S3.Stat3)	May 11, 2011	13	Maintained load	Capacity = 595 kN (37 mm)
(S3.Cyc1)	May 11, 2011	13	Cyclic load test (20 cycles)	0–440 kN (0 mm) (stable)
(S3.Cyc 2)	May 31, 2011	33	Cyclic load test (83 cycles)	0–580 kN (0.25 mm) (metastable)
(S3.Stat4)	October 19, 2012	540	Maintained load	Capacity = 1,192 kN (28 mm)
(S3.Stat5)	October 19, 2012	540	Maintained load	Capacity = 875 kN (8 mm)
S4	April 28, 2011	0	Driving (Junttan PM16)	529 blows (400-mm drop height)
(S4.Stat1)	May 31, 2011	33	Maintained load	Capacity = 385 kN (42 mm)
(S4.Stat1)	May 31, 2011	33	Quick maintained load	Capacity = 348 kN (30 mm)
(S4.Stat3)	July 29, 2011	92	Maintained load	Capacity = 520 kN (17 mm)
(S4.Stat4)	August 26, 2011	120	Maintained load	Capacity = 462 kN (24 mm)
(S4.Stat5)	August 26, 2011	120	Maintained load	Capacity = 450 kN (17 mm)
(S4.Cyc1)	August 26, 2011	120	Cyclic load test (105 cycles)	0–300 kN (<0.1 mm)
(S4.Cyc2)	August 26, 2011	120	Cyclic load test (105 cycles)	0–350 kN (0.6 mm)
(S4.Cyc3)	August 26, 2011	120	Cyclic load test (18 cycles)	0–400 kN (63 mm)
S5	April 28, 2011	0	Driving (Junttan PM16)	630 blows (400-mm drop height)
(S5.MLT1)	December 4, 2011	220	Maintained load	Capacity = 990 kN (20 mm)
S6	May 28, 2012	0	Driving (Junttan PM20)	1,501 blows (200–300 mm drop height)
(S6.Stat1)	September 21, 2012	116	Maintained load	Capacity = 1,050 kN (28 mm)
(S6.Stat2)	September 24, 2012	119	Quick load	Capacity = 870 kN (20 mm)
(S6.Cyc1)	September 25, 2012	120	Cyclic load test (400 cycles)	0–300 kN (0.05 mm)
(S6.Cyc2)	September 26, 2012	121	Cyclic load test (100 cycles)	0–400 kN (0.1 mm)
(S6.Cyc3)	September 26, 2012	121	Cyclic load test (750 cycles)	0–520 kN (1.8 mm)
(S6.Cyc4)	September 27, 2012	122	Cyclic load test (8 cycles)	0–620 kN (20 mm)
(S6.Stat3)	September 27, 2012	122	Quick load	Capacity = 620 kN (19 mm)

Note: Bold values are pile names and therefore act as headers for pile tests.

The tension static load tests were performed by Lloyds Acoustics Ltd. using a 5-m loading frame that transferred the load through reaction beams positioned ≈2.5 m from the test pile (Fig. 5). A steel top cap, welded onto the piles after installation, allowed the piles to be pulled using a threaded bar. Loads were measured using hollow load cells on top of the reaction frame, and pile head displacements were measured using four linear variable differential transformers (LVDTs). The static tension tests were performed using a fully automated load controlled hydraulic system that maintained each target load level for a specified time period. Typically for every first-time tension load test conducted, a second quick load test was conducted immediately following in order to assess the damage caused by the first load test on the pile capacity. As a result, the precyclic load test capacity of each pile could be accurately assessed. During the first-time tension tests on each pile, the pile was loaded in increments of 40 kN, with each load level maintained for 10 min. In subsequent standard reload tests, the load increments were maintained for approximately 5 min except for the "quick" reload tests (Table 1), which typically held each 40-kN increment for ≈1 min. The length of the maintained load hold periods did not appear to have a significant influence on the load-displacement response, in agreement with the findings of Jardine and Standing (2012).

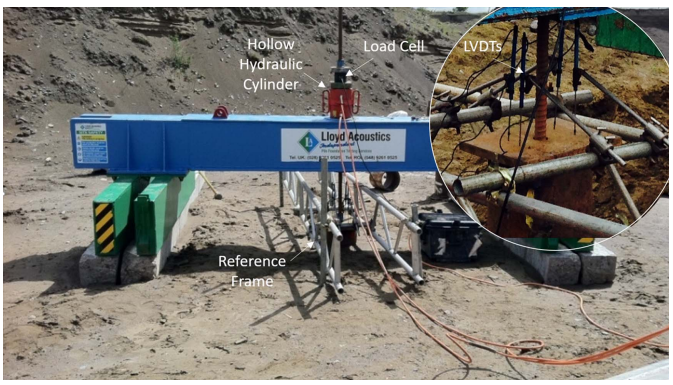

Fig. 5. Load test setup. (Image by David Igoe.)

Cyclic load tests were applied using a specially fabricated cyclic loading unit that consisted of an electronically controlled two-way hydraulic actuator with pressure control and release valves, powered by an electric motor. The cyclic setup was programmed to ramp between predetermined hydraulic pressures (loads) with fixed

cyclic periods of 10 s (0.1 Hz), which is typical for offshore environmental loading (Jardine et al. 2012).

Results of Repeated Static Load Testing

The results of the multiple static reload tests on each pile are described in this section. Pile S2 was initially load tested 1 day after driving and was used as the reference pile for the 1-day capacity. The complete load-displacement response for all tests conducted on Pile S2 is shown in Fig. 6(a). Multiple static tension tests to failure 1 day after installation (S2.Stat 1–3) did not result in any reduction in pile capacity, indicating that the 1-day capacity $Q_{s,1\text{-day}}$ may represent a lower-bound limit for the pile capacity. Static tension tests on the same pile conducted after an ageing period of 11 and 125 days (S2.Stat4 and Stat5) showed an increase in capacity due to ageing; however, the capacities remained lower than fresh piles, indicating that performing multiple tests to failure on the

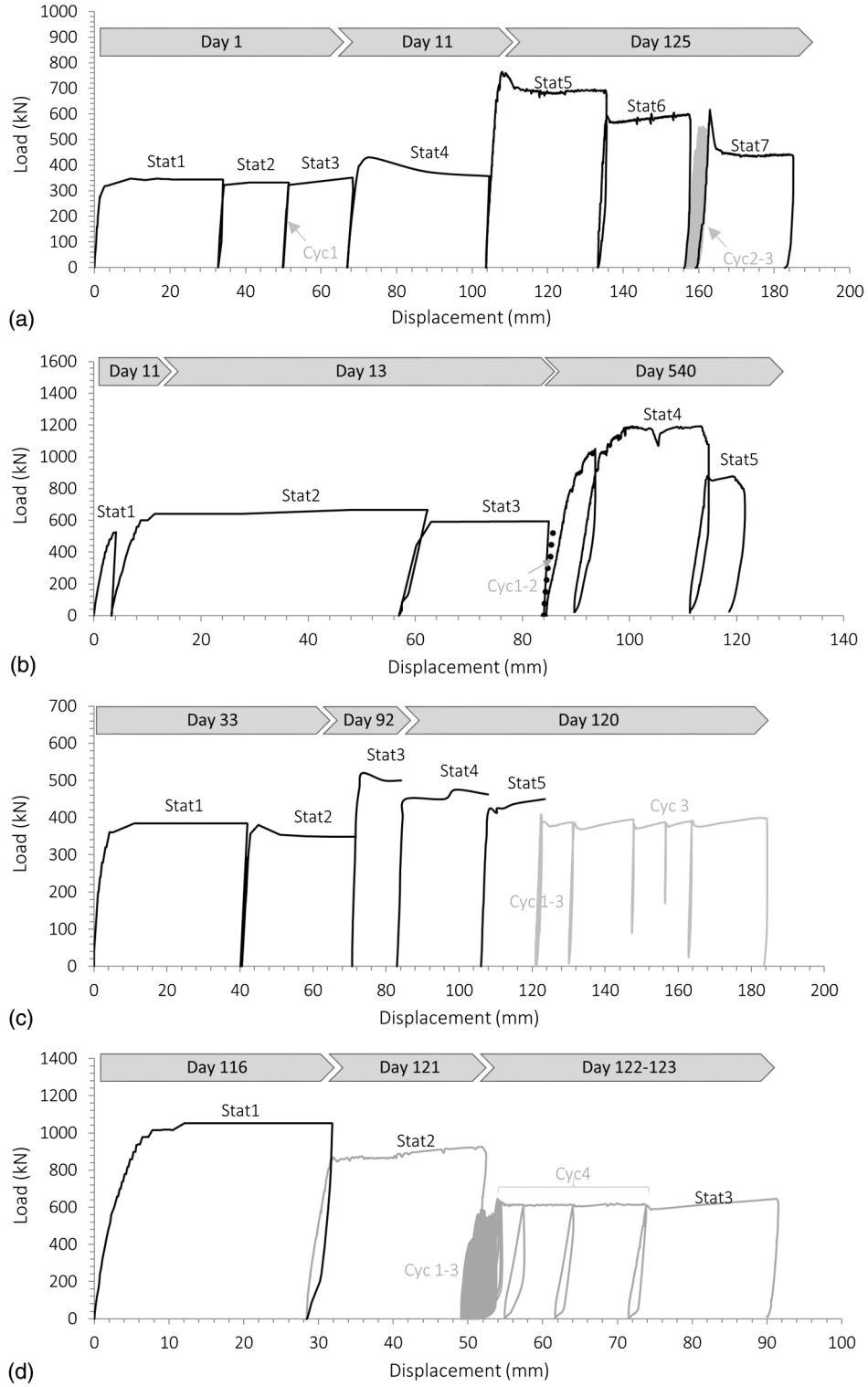

Fig. 6. Load-displacement response for all load tests for piles: (a) S2; (b) S3; (c) S4; and (d) S6.

same pile had reduced the ageing effect. Two further static tension tests performed at 125 days (S2.Stat6 and Stat7) to assess the effect of the retesting on the aged pile capacity showed a significant reduction in pile capacity, with the final capacity only 30% higher than $Q_{s,1\text{-day}}$. The findings from Pile S2 indicate that cyclic degradation only affects the ageing component of pile capacity ($Q_{s,\text{ageing}} = Q_{s(t)} - Q_{s,1\text{-day}}$).

Multiple static tests performed on Piles S3, S4, and S6 are provided in Figs. 6(b–d), respectively, and show the same trends for increase in capacity due to ageing and reduction in capacity due to static testing to failure. Further discussion and interpretation of the static test results are provided in the following sections.

Results of Cyclic Load Testing

The results of the cyclic load tests on all piles are presented in Fig. 7, where the applied head load (gray lines) and displacement (black lines) are plotted against cumulative number of cycles. A summary of the cyclic tests including load levels and pretest capacities is

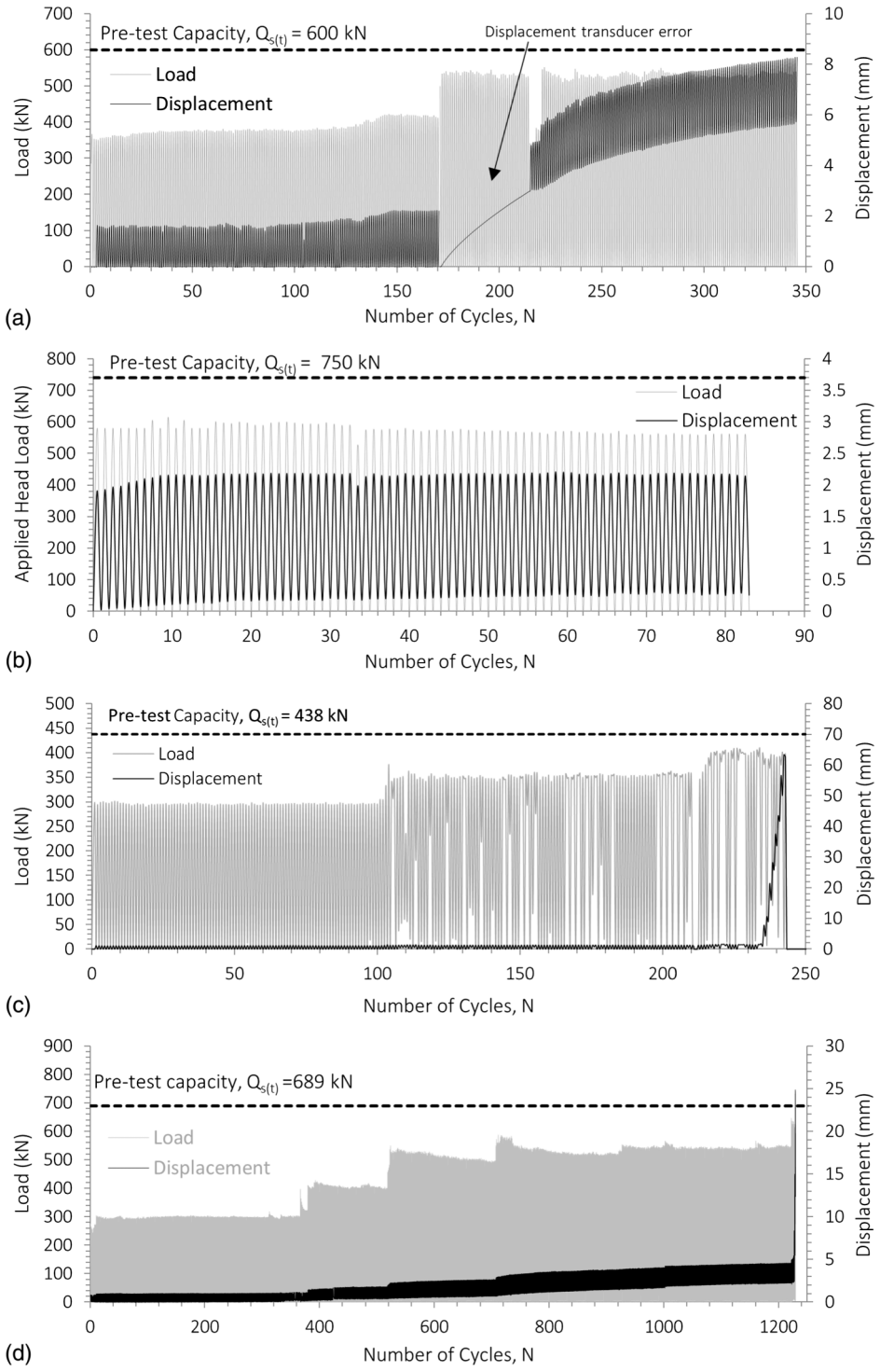

Fig. 7. Cyclic load tests: (a) Pile S2.Cyc2-3; (b) S3.Cyc2; (c) S4.Cyc 1-3; and (d) S6.Cyc 1-3.

Table 2. Blessington cyclic tests

Test No.	$Q_{s,1\text{-day}}$ (kN)	$Q_{s,\text{measured}}$ (kN)	$Q_{s,\text{ageing}}$ (kN)	$Q_{s(t)}$ (kN)	$Q_{\text{mean}}/Q_{s(t)}$	$Q_{\text{cyc}}/Q_{s(t)}$	N_f	Stability
S2.Cyc1	338	340	2	339	0.32	0.32	No failure	Stable
S2.Cyc2	338	600	262	600	0.33	0.33	No failure	Stable
S2.Cyc3	338	600	262	600	0.43	0.43	No failure	Metastable
S3.Cyc2	347	595	248	751	0.38	0.38	No failure	Metastable
S4.Cyc1	337	450	113	438	0.34	0.34	No failure	Stable
S4.Cyc2	337	450	113	438	0.40	0.40	No failure	Metastable
S4.Cyc3	337	450	113	438	0.46	0.46	18	Unstable
S6.Cyc1	343	870	527	689	0.22	0.22	No failure	Stable
S6.Cyc2	343	870	527	689	0.29	0.29	No failure	Stable
S6.Cyc3	343	870	527	689	0.38	0.38	No failure	Metastable
S6.Cyc4	343	870	527	689	0.45	0.45	8	Unstable

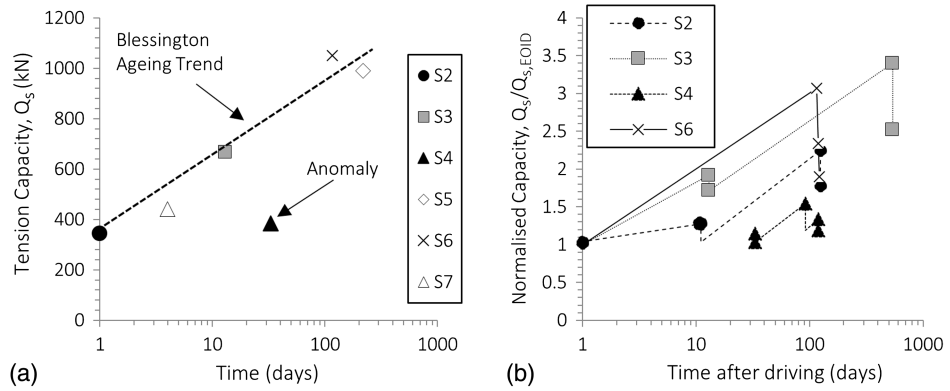

Fig. 8. (a) Blessington intact ageing trend from (data from Gavin and Igoe 2019); and (b) the effect of static failures on ageing of Piles S2–S6.

provided in Table 2. The cyclic behavior of the test piles is described in terms of stable, metastable, and unstable behavior. The majority of cyclic tests exhibited stable behavior with no accumulated displacements or failure. Three tests, S2.Cyc3, S4.Cyc2, and S6.Cyc3, exhibited apparent metastable behavior, where displacements continue to accumulate, but were not cycled long enough to reach failure. A problem with the displacement transducers during S2.Cyc3 resulted in some data loss for the first 50 load cycles, but an estimate of the initial displacements based on the remaining load cycles suggests a metastable loading response with ≈3 mm of permanent displacement accumulated during the test. Only two cyclic tests, S4.Cyc3 and S6.Cyc4, were cycled to failure, where capacity reduction led to large plastic displacements.

Discussion

Interpretation of Pile Ageing and Static Testing to Failure

By performing a comprehensive load test program involving multiple static and cyclic tension load tests on four separate piles, the effects of ageing and cyclic loading on the piles were accurately assessed. Fig. 8(a) shows an intact ageing trend from the untested fresh pile tension capacities, previously described in Gavin and Igoe (2019). It is clear that Pile S4 is an outlier, where the capacity falls significantly below the intact ageing trend. Fig. 8(b) shows the pile tension capacities for all static tests described in this paper normalized by their respective 1-day capacity $Q_{s,1\text{-day}}$. Because only Pile S2 was load tested 1 day after driving, and in order to account for soil variability between the piles, $Q_{s,1\text{-day}}$ was calculated for each pile using the CPT-based UWA-05 axial pile design method (Lehane et al. 2005) and applying an ageing factor of 0.65 to account for the reduced capacity 1 day after driving. The UWA-05 method was favored over other methods, such as the ICP-05 method (Jardine et al. 2005), due to its ability to account for partial plugging through the IFR term and its excellent match with the 1-day capacity from Pile S2 ($Q_{s,\text{UWA}} \times 0.65/Q_{s,\text{measured}} = 0.99$).

For aged piles, multiple static load tests to failure can result in significant capacity degradation. However, for piles that have not experienced capacity increases due to ageing, no decrease in capacity was noted, as seen from the multiple static failures performed on Pile S2 1 day after driving. This would suggest that the 1-day tension capacity $Q_{s,1\text{-day}}$ represents a lower-bound capacity for cyclic degradation. This seems logical, considering: (1) the dynamic shear stress cycles imposed during pile driving are likely to be significantly more severe than those during in-service cyclic loading, and (2) the radial stress reduction due to principal stress rotations that occur during tension static loading is not likely to be amplified by cyclic loading. In all cases, even after severe cyclic loading and multiple failures, the capacity of the piles never dropped below the reference 1-day capacity. Similar behavior at Dunkirk was noted by Jardine et al. (2006) and Jardine and Standing (2012).

Even after the piles had experienced multiple failures, large capacity increases due to ageing were noted. The slopes of the normalized capacity–time plots [Fig. 8(b)] were similar between fresh and prefailed piles, the difference being that each failure on an aged pile caused significant reductions in the aged capacity. One exception to this was the rate of capacity growth for Pile S2 over the first 11 days after driving. In order to quantify the shaft capacity degradation caused by large displacement single-cycle static failures on aged piles, the capacity change measured between two

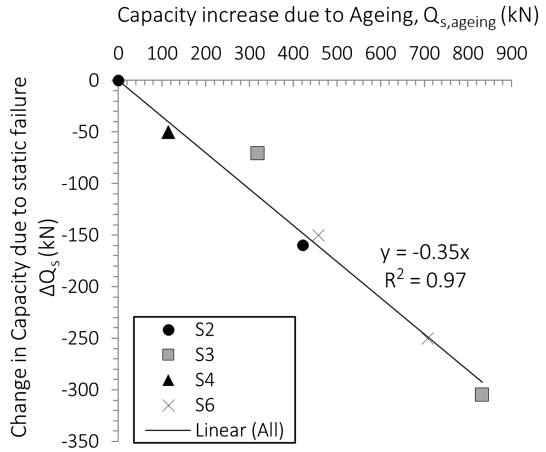

Fig. 9. Decrease in capacity due to repeated static load tests to failure compared with pretest capacity increases due to ageing.

consecutive static failures (ΔQ_s) is plotted against the pretest capacity gains due to ageing ($Q_{s,\text{ageing}}$) in Fig. 9. A linear trend-line provides an excellent fit to the data and suggests a strong correlation between capacity degradation and ageing, such that each single-cycle static test caused an average 35% drop in the ageing component of the capacity:

$$\Delta Q_s = -0.35 \times Q_{s,\text{ageing}} = -0.35 \times (Q_{s(t)} - Q_{s,\text{1-day}}) \quad (4)$$

However, after two successive failures (with no ageing in between), no further capacity reductions were seen to occur, as was the case for Piles S4 and S6. Similar reductions in the aged pile tension capacity were noted during two consecutive tension load tests on Pile R6 at Dunkirk (Jardine and Standing 2000).

Interpretation of Cyclic Tests

In light of the previous observations, the $Q_{s(t)}$ values from the Dunkirk load tests were reinterpreted on the basis that a static load test would result in an average 35% drop in the aged component of pile capacity. In the cases where the static load test immediately preceding cyclic loading did not reach failure, or where there was a significant ageing period between static testing and cyclic loading, the best estimate $Q_{s(t)}$ values originally proposed by Jardine and Standing (2012) were used. Table 3 provides the new reinterpreted $Q_{s(t)}$ values compared with the original values. The reinterpreted Dunkirk data (square symbols) and new Blessington test data (circle symbols) were compared with cyclic interaction diagrams proposed by Jardine and Standing (2012) in Fig. 10. The data are plotted as the mean (Q_{mean}) and cyclic (Q_{cyc}) amplitudes normalized by the available tension capacity $Q_{s(t)}$ (accounting for the effects of prefailure) with stable behavior noted by open symbols, metastable with gray symbols, and unstable with black symbols. Despite the difference in the sand state and pile geometry (and therefore pile capacities) at the two sites, the data are remarkably consistent. The new data suggest the boundary lines proposed by Jardine and Standing (2012) are slightly conservative and new boundary lines, 15%–20% higher, appear to offer a better fit to the data.

In order to calculate the global degradation due to cyclic loading, the approach proposed by Jardine and Standing (2012) in Eq. (3) can be modified to account for the new findings in this paper by including a normalized ageing term as follows:

$$\frac{\Delta Q_s}{Q_{s(t)}} = a\left(\frac{Q_{s,\text{ageing}}}{Q_{s(t)}}\right)\left(b + \frac{Q_{\text{cyc}}}{Q_{s(t)}}\right)N^c \quad (5)$$

The average $Q_{s,\text{ageing}}/Q_{s(t)}$ for original Dunkirk piles was 0.54, and therefore adopting values of $a = -0.234$, $b = -0.1$, and $c = 0.45$ will match the original Eq. (1) calibration well. For one-way cycling where $Q_{\text{cyc}} = Q_{\text{mean}}$, failure will occur when $\{(\Delta Q_s)/[Q_{s(t)}]\} = 2\{(Q_{cyc})/[Q_{s(t)}]\} - 1$, and therefore Eq. (5) can be rearranged to calculate the number of cycles to failure as follows:

$$N_f = \left[\frac{\left(2\frac{Q_{\text{cyc}}}{Q_{s(t)}} - 1\right)}{a\left(\frac{Q_{s,\text{ageing}}}{Q_{s(t)}}\right)\left(b + \frac{Q_{\text{cyc}}}{Q_{s(t)}}\right)}\right]^{\frac{1}{c}} \quad (6)$$

Direct calibration against the Dunkirk and Blessington field test results was undertaken using constrained optimization, minimizing the square of the difference between the calculated and measured N_f values for each cyclic test. The calibration gives the following values: $a = -0.206$, $b = -0.100$, and $c = 0.390$. The combined contribution of number of cycles, cyclic amplitude, and ageing using Eq. (5) to predict cyclic degradation can be visualized using a three-dimensional (3D) surface plot, as shown in Fig. 11. The different surfaces in the plot represent different levels of ageing contribution to pretest capacity. Standard axial pile design methods, such as the ICP-05 and UWA-05 design approaches, are calibrated to predict the medium-term (10–30-day) capacity. Although these methods do not explicitly consider ageing affects in the standard calculations, they have an inherent ageing component $Q_{s,\text{ageing}}/Q_{s(t)} \approx 0.33$ based on their calibration, which is the top dark gray

Table 3. Re-interpretation of Dunkirk cyclic tests

Test No.	$Q_{s,\text{1-day}}$ (kN)	$Q_{s,\text{measured}}$ (kN)	$Q_{s,\text{ageing}}$ (kN)	$Q_{s(t)}$ old (kN)	$Q_{s(t)}$ new (kN)	$Q_{\text{mean}}/Q_{s(t)}$	$Q_{\text{cyc}}/Q_{s(t)}$	Stability	N_f
2.C1.CY3	437	820	259	840	**696**	−0.06	0.86	Unstable	41
2.C1.CY5	437	696	181	620	**619**	0.02	0.66	Unstable	12
3.R2.CY2	904	3,210	1,499	2,500	**2,403**	0.42	0.42	Unstable	9
2.R3.CY2	930	2,315	1,078	2,315	**2,008**	0.35	0.35	Metastable	200
2.R3.CY3	930	2,315	1,121	2,050	2,050	0.46	0.46	Unstable	13
2.R4.CY2	1,105	2,000	1,858	2,963	2,963	0.34	0.34	Metastable	221
2.R4.CY4	1,105	2,000	995	2,100	2,100	0.60	0.36	Unstable	3
3.R4.CY6	1,105	2,100	1,005	2,110	2,110	0.19	0.19	Stable	No failure
2.R5.CY2	923	2,000	1,542	2,465	2,465	0.41	0.41	Metastable	345
2.R5.CY3	923	2,000	720	2,000	**1,643**	0.43	0.43	Unstable	27
2.R6.CY2	826	2,450	1,175	2,000	2,000	0.63	0.38	Unstable	1
2.R6.CY4	826	1,585	760	1,585	1,585	0.44	0.44	Unstable	24
3.R6.CY6	826	1,325	825	1,650	1,650	0.42	0.42	Metastable	206

Note: Bold values are changes from old interpretation.

J. Geotech. Geoenviron. Eng., 2021, 147(4): 04021011

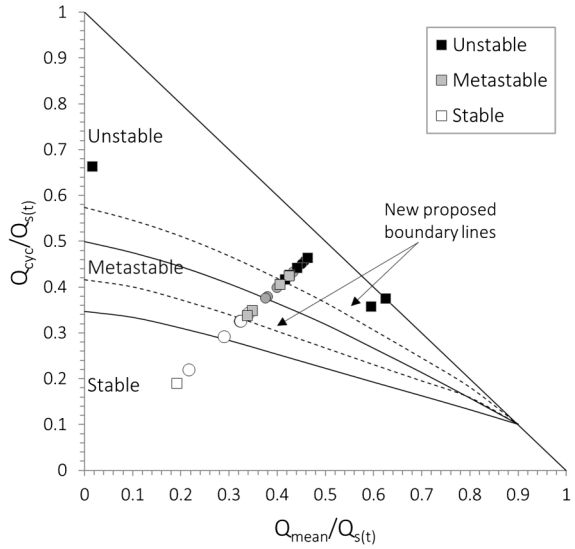

Fig. 10. Combined Blessington (circle markers) and Dunkirk (square markers) cyclic load tests with cyclic interaction diagrams proposed for Dunkirk (solid lines) and new proposed boundaries (dashed lines).

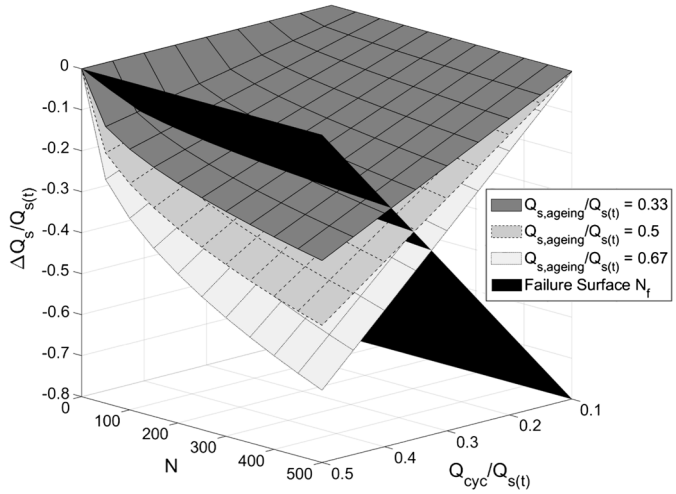

Fig. 11. Normalized capacity degradation surfaces for different levels of ageing using Eq. (4).

surface shown in Fig. 11. Piles designed with larger ageing components $Q_{s,\text{ageing}}/Q_{s(t)} = 0.5$ and 0.67 are also shown, along with the cut-off surface representing the number of cycles to failure from Eq. (6) (black surface). It is clear from the figure that the rate of capacity degradation is highly dependent on the ageing and that cyclic capacity degradation for piles that are designed without ageing effects may be significantly lower than currently considered.

Summary and Conclusions

This paper presents results from a series of field-scale pile load tests at the geotechnical research test site in Blessington, Ireland. The tests were performed to examine the effects of ageing and cyclic loading on the axial shaft capacity of piles in sand. Four steel piles were subjected to more than 30 tension load tests, and the testing schedule was organized so as to fill in the gaps in previous testing programs from the literature. The following are the key conclusions:

1. All the piles indicated significant capacity increases over time. Aged piles that were load tested to failure showed significant capacity degradation but generally regained capacity at similar rates of ageing to previously untested fresh piles.
2. Multiple static tension load tests to failure performed 1 day after driving did not result in any capacity reductions, indicating the 1-day tension capacity represents a lower-bound capacity for cyclic degradation. Tension tests performed on various piles in the weeks and months after driving all indicated large drops in the capacity due to failure during static loading but never dropped below the 1-day capacity.
3. The capacity reduction measured in multiple sequential static load tests showed a strong linear correlation with the capacity gains due to ageing, indicating that cyclic degradation should also be linked to pile capacity gains due to ageing.
4. A reinterpretation of previous cyclic testing on aged piles, along with the new tests, was used to develop new boundaries for cyclic interaction diagrams. An updated global approach to cyclic degradation, which includes an ageing component, was proposed and highlights the conservatism within existing design.

The results discussed in this paper are particularly important considering the inherent ageing factors in standard pile design calculations and the large safety factors employed in practice.

Data Availability Statement

All data, models, and code generated or used during the study appear in the published article.

Acknowledgments

The authors wish to express their gratitude to Mainstream Renewable Power, the Irish Research Council for Science and Technology (IRCSET) and Enterprise Ireland (Grant No. IP/2010/0085), and Science Foundation Ireland (through Grant No.10-RFP-GEO2895) for cofinancing these field tests. The test piles were installed by Bullivan Tarranto, and pile testing was undertaken by Lloyd Acoustics Ltd. and UCD. The authors thank Roadstone Ltd. for permission to use the Redbog quarry at Blessington for the field tests. In-situ testing was performed by In-Situ SI Ltd., and thanks are due to the following research staff and students at UCD for assisting in the fieldwork: Dr. Lisa Kirwan and Mr. Tim Hennessey.

Notation

The following symbols are used in this paper:

A = coefficient for Eq. (2);
a = coefficient for Eq. (4);
B = coefficient for Eq. (2);
b = coefficient for Eq. (4);
C = coefficient for Eq. (2);
c = coefficient for Eq. (4);
D = pile outer diameter, m;
D_{50} = mean particle size, mm;
N = number of load cycles;
$Q_{s,\text{ageing}}$ = increase in shaft capacity due to ageing, kN;
Q_{cyc} = cyclic load amplitude, kN;
Q_{mean} = mean cyclic load, kN;

$Q_{s(t)}$ = static shaft capacity available preceding load test, kN;
$Q_{s,\text{measured}}$ = measured shaft capacity in static load test, kN;
q_c = CPT cone resistance, MPa;
t = time after pile installation, days;
$\Delta\sigma'_r$ = change in local shaft radial stress due during loading;
$\Delta\sigma'_{r,\text{cyc}}$ = change in shaft radial stress due to cyclic loading;
δ_f = interface friction angle at failure;
σ'_{rc} = local equalized radial effective stress at failure, kPa;
σ'_{rf} = local shaft radial effective stress at failure, kPa;
τ_f = shaft shear stress at failure; and
τ_{cyc} = locally applied cyclic shear stress.

References

Axelsson, G. 2000. "Long-term setup of driven piles in sands." Ph.D. dissertation, Dept. of Civil and Environmental Engineering, Royal Institute of Technology.

Baxter, C. D. P., and J. K. Mitchell. 2004. "Experimental study on the aging of sands." *J. Geotech. Geoenviron. Eng.* 130 (10): 1051–1062. https://doi.org/10.1061/(ASCE)1090-0241(2004)130:10(1051).

Bullock, P. J., J. H. Schmertmann, M. C. McVay, and F. C. Townsend. 2005. "Side shear setup. I: Test piles driven in Florida." *J. Geotech. Geoenviron. Eng.* 131 (3): 292–300. https://doi.org/10.1061/(ASCE)1090-0241(2005)131:3(292).

Carroll, R., P. Carotenuto, C. Dano, I. Salama, M. Silva, S. Rimoy, K. Gavin, and R. Jardine. 2019. "Field experiments at three sites to investigate the effects of age on steel piles driven in sand." *Géotechnique* 70 (6): 469–489. https://doi.org/10.1680/jgeot.17.P.185.

Chow, F., R. J. Jardine, F. Brucy, and J. Nauroy. 1998. "Effects of time on capacity of pipe piles in dense marine sand." *J. Geotech. Geoenviron. Eng.* 124 (Mar): 254–264. https://doi.org/10.1061/(ASCE)1090-0241(1998)124:3(254).

Doherty, P., L. Kirwan, K. G. Gavin, D. Igoe, S. Tyrrell, D. Ward, and B. C. O'Kelly. 2012. "Soil properties at the UCD geotechnical research site at Blessington." In *Proc., Bridge and Concrete Research in Ireland 2012*. Dublin, Ireland: Civil Engineering Research Association of Ireland.

Dumas, J. C., and N. F. Beaton. 1988. "Discussion of 'practical problems from surprising soil behavior' by James K. Mitchell (March, 1986, Vol. 112, No. 3)." *J. Geotech. Eng.* 114 (3): 367–368. https://doi.org/10.1061/(ASCE)0733-9410(1988)114:3(367).

Flynn, K., and B. A. Mccabe. 2016. "Energy transfer ratio for hydraulic pile driving hammers." In *Proc., Civil Engineering Research in Ireland Conf.* Dublin, Ireland: Civil Engineering Research Association of Ireland.

Gavin, K. G., and D. Igoe. 2019. "A field investigation into the mechanisms of pile ageing in sand." *Géotechnique* 1–12. https://doi.org/10.1680/jgeot.18.P.235.

Gavin, K. G., D. Igoe, and L. Kirwan. 2013. "The effect of ageing on the axial capacity of piles in sand." *Proc. Inst. Civ. Eng. Geotech. Eng.* 166 (2): 122–130.

Gavin, K. G., R. Jardine, K. Karlsrud, and B. Lehane. 2015. "The effects of pile ageing on the shaft capacity of offshore piles in sand." In *Proc., Frontiers in Offshore Geotechnics III*, 129–151. Milton Park, UK: Taylor and Francis.

Igoe, D., and K. Gavin. 2019. "Characterization of the Blessington sand geotechnical test site." *Aims Geosci.* 5 (Apr): 145–162. https://doi.org/10.3934/geosci.2019.2.145.

Igoe, D., K. Gavin, and L. Kirwan. 2013. "Investigation into the factors affecting the shaft resistance of driven piles in sands." In *Proc., Int. Conf. on Installation Effects in Geotechnical Engineering*. Rotterdam, Netherlands: A.A. Balkema.

Igoe, D., K. G. Gavin, and B. C. O'Kelly. 2011. "Shaft capacity of open-ended piles in sand." *J. Geotech. Geoenviron. Eng.* 137 (10): 903–913. https://doi.org/10.1061/(ASCE)GT.1943-5606.0000511.

Jardine, R., F. Chow, R. Overy, and J. Standing. 2005. *ICP design methods for driven piles in sands and clays*. London: Thomas Telford.

Jardine, R., A. Puech, and K. H. Andersen. 2012. "Cyclic loading of offshore piles: Potential effects and practical design." In *Proc., 7th Int. Conf. Offshore Site Investigation and Geotechnics 2012: Integrated Technologies—Present and Future*, 59–97. London: Society for Underwater Technology.

Jardine, R., and J. Standing. 2000. *Pile load testing performed for HSE cyclic loading study at Dunkirk, France: Volume 1&2*. Offshore Technology Rep. No. OTO 7. London: Health and Safety Executive.

Jardine, R. J., and F. C. Chow. 2007. "Some recent developements in offshore pile design." In *Proc., 6th Int. Offsore Site Investigations and Geotechnics Conf.*, 303–332. London: Society for Underwater Technology.

Jardine, R. J., and J. R. Standing. 2012. "Field axial cyclic loading experiments on piles driven in sand." *Soils Found.* 52 (4): 723–736. https://doi.org/10.1016/j.sandf.2012.07.012.

Jardine, R. J., J. R. Standing, and F. C. Chow. 2006. "Some observations of the effects of time on the capacity of piles driven in sand." *Géotechnique* 56 (4): 227–244. https://doi.org/10.1680/geot.2006.56.4.227.

Jefferies, M. G., B. T. Rogers, H. R. Stewart, S. Shinde, D. J. Williams-Fitzpatrick, and S. Williams-Fitzpatrick. 1988. "Island construction in the Canadian Beaufort Sea." In *Hydraulic fill structures*, 816–883. Reston, VA: ASCE.

Lehane, B. M., R. J. Jardine, A. J. Bond, and R. Frank. 1993. "Mechanisms of shaft friction in sand from instrumented pile tests." *J. Geotech. Eng.* 119 (1): 19–35. https://doi.org/10.1061/(ASCE)0733-9410(1993)119:1(19).

Lehane, B. M., J. A. Schneider, and X. Xu. 2005. "The UWA-05 method for prediction of axial capacity of driven piles in sand." In *Proc., Int. Symp. on Frontiers in Offshore Geotechnics (IS-FOG 2005)*, 683–689. Milton Park, UK: Taylor and Francis.

Lim, J. K., and B. Lehane. 2015. "Time effects on the shaft capacity of jacked piles in sand." *Can. Geotech. J.* 1838 (Apr): 1–38.

Manceau, S., V. Thurmann, A. Sia, and R. McLean. 2019. "Mitigating pile driving refusal risk for a North Sea offshore wind farm through design and installation planning." In *Proc., XVII ECSMGE-2019*, 1–8. London: International Society for Soil Mechanics and Geotechnical Engineering. https://doi.org/10.32075/17ECSMGE-2019-0755.

Mesri, G., T. W. Feng, and J. M. Benak. 1990. "Postdensification penetration resistance of clean sands." *J. Geotech. Eng.* 116 (7): 1095–1115. https://doi.org/10.1061/(ASCE)0733-9410(1990)116:7(1095).

Mitchell, J. K., and S. V. Solymar. 1984. "Time-dependent strength gain in freshly deposited or densified sand." *J. Geotech. Eng.* 110 (11): 1559–1576. https://doi.org/10.1061/(ASCE)0733-9410(1984)110:11(1559).

Puech, A., O. Benzaria, L. Thorel, J. Garnier, P. Foray, M. Silva, and R. Jardine. 2013. "Cyclic stability diagrams for piles in sands." In *Proc., TC 209 Workshop—18th ICSMGE, Paris 4 September 2013 Design for Cyclic Loading: Piles and Other Foundations*, 85–88. Paris: Presses des Pontes.

Rimoy, S., M. Silva, R. Jardine, Z. Yang, B. Zhu, and C. Tsuha. 2015. "Field and model investigations into the influence of age on axial capacity of displacement piles in silica sands." *Géotechnique* 65 (7): 576–589. https://doi.org/10.1680/geot.14.P.112.

Rimoy, S. P., R. J. Jardine, and J. R. Standing. 2013. "Displacement response to axial cycling of piles driven in sand." *Proc. Inst. Civ. Eng. Geotech. Eng.* 166 (2): 131–146. https://doi.org/10.1680/geng.12.00052.

Schmertmann, B. J. H. 1992. "The mechanical aging of soils." *J. Geotech. Eng.* 117 (9): 1288–1330. https://doi.org/10.1061/(ASCE)0733-9410(1991)117:9(1288).

Tsuha, C. H. C., P. Y. Foray, R. J. Jardine, Z. X. Yang, M. Silva, and S. Rimoy. 2012. "Behaviour of displacement piles in sand under cyclic axial loading." *Soils Found.* 52 (3): 393–410. https://doi.org/10.1016/j.sandf.2012.05.002.

White, D. J. 2005. "A general framework for shaft resistance on displacement piles in sand." *Proc., 1st Int. Symp. on Frontiers in Offshore Geotechnics*, 697–703. Milton Park, UK: Taylor and Francis.

White, D. J., and M. D. Bolton. 2001. "Displacement and strain paths during plane–strain model pile installation in sand." *Géotechnique* 54 (6): 375–397. https://doi.org/10.1680/geot.2004.54.6.375.
Yang, Z. X., R. J. Jardine, B. T. Zhu, P. Foray, and C. H. C. Tsuha. 2010. "Sand grain crushing and interface shearing during displacement pile installation in sand." *Géotechnique* 60 (6): 469–482. https://doi.org/10.1680/geot.2010.60.6.469.
York, D. L., W. G. Brusey, F. M. Clemente, and S. K. Law. 1994. "Setup and relaxation in glacial sand." *J. Geotech. Eng.* 120 (9): 1498–1513. https://doi.org/10.1061/(ASCE)0733-9410(1994)120:9(1498).